Journal of Experimental Botany, Vol. 62, No. 2, pp. 627–640, 2011
doi:10.1093/jxb/erq314 Advance Access publication 26 October, 2010
This paper is available online free of all access charges (see http://jxb.oxfordjournals.org/open_access.html for further details)

Journal of Experimental Botany
www.jxb.oxfordjournals.org

RESEARCH PAPER

Role of relative humidity, temperature, and water status in dormancy alleviation of sunflower seeds during dry after-ripening

J. Bazin[1], D. Batlla[2], S. Dussert[3], H. El-Maarouf-Bouteau[1] and C. Bailly[1,*]

[1] UPMC Université Paris 06, UR5 UPMC - EAC 7180 CNRS, Bat C, 2ème étage, boîte 156, 4, place Jussieu, F-75252 Paris cedex 05, France

[2] IFEVA/Cátedra de Cerealicultura, CONICET/Facultad de Agronomía, Universidad de Buenos Aires, Av. San Martín 4453, C1417DSE-Buenos Aires, Argentina

[3] IRD, UMR DIA-PC, 911 Av. Agropolis, BP64501, F-34394 Montpellier, France

* To whom correspondence should be addressed. E-mail: christophe.bailly@upmc.fr

Received 1 July 2010; Revised 27 August 2010; Accepted 3 September 2010

Abstract

The effect of various combinations of temperature and relative humidity on dormancy alleviation of sunflower seeds during dry after-ripening was investigated. The rate of dormancy alleviation depended on both temperature and embryo moisture content (MC). Below an embryo MC of 0.1 g H_2O g^{-1} dw, dormancy release was faster at 15 °C than at higher temperatures. This suggests that dormancy release at low MC was associated with negative activation energy, supported by Arrhenius plots, and low Q_{10} values. At higher MC, the rate of dormancy alleviation increased with temperature, correlating well with the temperature dependence of biochemical processes. These findings suggests the involvement of two distinct cellular mechanisms in dormancy release; non-enzymatic below 0.1 g H_2O g^{-1} dw and associated with active metabolism above this value. The effects of temperature on seed dormancy release above the threshold MC were analysed using a population-based thermal time approach and a model predicting the rate of dormancy alleviation is provided. Sunflower embryo dormancy release was effective at temperatures above 8 °C (the base temperature for after-ripening, Tb_{AR}, was 8.17 °C), and the higher the after-ripening temperature above this threshold value, the higher was the rate of dormancy loss. Thermodynamic analyses of water sorption isotherms revealed that dormancy release was associated with less bound water and increased molecular mobility within the embryonic axes but not the cotyledons. It is proposed that the changes in water binding properties result from oxidative processes and can, in turn, allow metabolic activities.

Key words: After-ripening, physiological dormancy, relative humidity, seed, sunflower, temperature, thermal time, water status.

Introduction

After-ripening is the process by which freshly harvested mature seeds become non-dormant, i.e. they acquire the ability to germinate after a prolonged period of storage in dry conditions. After-ripening mainly results in a widening of the environmental conditions (temperature, light, oxygen availability) that allow germination and in an increase in germination speed (Probert, 2000; Finch-Savage and Leubner-Metzger, 2006). Seed after-ripening is a mechanism common to many, but not all, species. Other mechanisms of dormancy alleviation include chilling in the hydrated state or scarification (Finch-Savage and Leubner-Metzger, 2006; Finkelstein *et al.*, 2008).

Both temperature and seed moisture content (MC) can alter the rate of dormancy alleviation during dry storage (see Probert, 2000, and references therein). Various studies have shown that seed dry after-ripening is effective at MCs from *c.* 5–18% (on a fresh weight basis) (Leopold *et al.*, 1988; Foley, 1994; Probert, 2000; Steadman *et al.*, 2003;

Bair *et al.*, 2006), suggesting that the mechanisms that alleviate dormancy are inoperative outside this MC window. Considering thermodynamic principles based on the analysis of water sorption isotherms, it has been proposed that dry after-ripening is favoured in region 2 of sorption isotherms, which corresponds to weakly bound water (Probert, 2000). The effect of seed MC on dormancy alleviation could be particularly relevant under natural conditions, in the soil seed bank, where environmental conditions may vary drastically (Batlla and Benech-Arnold, 2006, 2010). However, the mechanisms of dormancy alleviation have been scarcely studied during 'dry' after-ripening, when free water is theoretically not available in seed tissues.

Temperature is the other critical environmental factor that affects the status of dormancy during dry storage. In most species, dormancy is alleviated faster with increasing after-ripening temperature. This positive correlation of temperature and dormancy release is in agreement with the metabolic theory in ecology (Brown *et al.*, 2004), which postulates that the temperature dependence of most biological reaction rates obeys an Arrhenius relationship (Gillooly *et al.*, 2001; Brown *et al.*, 2004). Although the seed MC during dry after-ripening is too low to detect any measurable metabolism, the temperature coefficient Q_{10}, which quantifies the temperature dependence, has been demonstrated to be constant within a species with positive values varying from *c.* 2–4 (Probert, 2000). This thermal behaviour, i.e. the increase in the rate of dormancy alleviation with increasing temperature, allowed developing models that predict the required duration of after-ripening as a function of temperature (Favier, 1995; Christensen *et al.*, 1996; Steadman *et al.*, 2003; Chantre *et al.*, 2009). Many of those models used thermal-time equations to establish a quantitative relationship between temperature and dormancy release, and used population approaches, to incorporate the variation of dormancy level within a seed population (Allen *et al.*, 2007). Both approaches have been proven to be very efficient for characterizing and quantifying changes in seed dormancy level in relation to prevailing temperature for various species (Batlla and Benech-Arnold, 2007, 2010).

The relationship between temperature and MC and its combined effect on dormancy release has mainly been investigated during the stratification of imbibed seeds, for example, in *Aesculus hippocastanum* (Pritchard *et al.*, 1996), *Orobanche* (Kebreab and Murdoch, 1999), *Lolium rigidum* (Steadman, 2004) or grape (Wang *et al.*, 2009). However, this relationship remains elusive under conditions of dry after-ripening, when free water is theoretically not available (Vertucci and Farrant, 1995). Bair *et al.* (2006) proposed a hydrothermal after-ripening time model for *Bromus tectorum* seeds, suggesting that water potential affects dormancy loss in a restricted range of values. The cytoplasm of anhydrobiotic seeds vitrifies and forms glasses that prevent molecular diffusion and chemical reactions (Buitink *et al.*, 2004). Nonetheless, some biochemical processes have been shown to occur under these conditions and have been associated with seed dormancy release. Oracz *et al.* (2007) demonstrated that sunflower seed after-ripening was associated with reactive oxygen species (ROS) accumulation and protein carbonylation. Changes in gene expression, suggesting active transcription in the dry state, were also shown to occur during dry after-ripening of seeds of various species (Bove *et al.*, 2005; Leubner-Metzger, 2005; Cadman *et al.*, 2006; Leymarie *et al.*, 2007).

The purpose of this study was to investigate the relationship between temperature and moisture content during seed dry after-ripening of sunflower (*Helianthus annuus* L.) seeds, which are dormant at harvest and hardly germinate at low temperatures (10 °C) (Corbineau *et al.*, 1990). This inability to germinate at low temperature results from a physiological dormancy (embryo dormancy). It has previously been shown that storage of dormant sunflower seeds at very low relative humidity can prevent embryo dormancy release (Oracz *et al.*, 2007) thus suggesting a pivotal role for seed MC in the mechanisms of dormancy alleviation. Dormant seeds were therefore stored at a large range of temperatures and relative humidities and the rate of dormancy release was assessed. Expecting that the seed MC may control dormancy release, thermodynamic approaches, based on water sorption isotherm analyses, were also used to determine whether dormancy alleviation is associated with changes in water properties. Finally, to assess the effect of temperature during after-ripening, an after-ripening thermal time model was developed for primary dormancy release of sunflower seeds. Our data demonstrate that the relationship between temperature, seed MC, and rate of dormancy alleviation is more complex than previously thought. Our thermodynamic analyses show that water-binding properties change during dormancy alleviation towards less bound water being available and, in turn, that this change controls the nature of the reactions involved in the transition from the dormant to a non-dormant state.

Material and methods

Plant material and after-ripening conditions

Sunflower (*Helianthus annuus* L., cv. LG5665) seeds were harvested in 2005 near Montélimar (Drôme, France) and purchased from Limagrain. At harvest, dormant seeds were stored at –30 °C until use in order to maintain their dormancy. After-ripening was performed by placing the dormant seeds at 15, 20, 25, and 30 °C over saturated solutions of $ZnCl_2$, $KOOCCH_3$, $CaCl_2$, NaCl, and KCl (Table 1) in tightly closed jars with relative humidities (RH) of approximately 5, 23, 33, 75, and 85%, respectively (Vertucci and Roos, 1993; Sun, 2004). Controls for non-dormant embryos were obtained from seeds that had been stored for 12 weeks in ambient conditions (*c.* 20 °C and 70% RH).

Germination tests

Germination tests were performed with naked seeds (i.e. seeds without pericarp), hereafter referred to as 'embryos', in darkness in 9 cm Petri dishes (25 embryos per dish, eight

Table 1. Relative humidities obtained using various saturated salt solutions at different temperatures (from Vertucci and Roos, 1993; Sun, 2004)

Saturated salt solution	Relative humidity (%) at				
	5 °C	15 °C	20 °C	25 °C	30 °C
P_2O_5	0.5	0.5	–	0.5	–
$ZnCl_2$	5.5	5.5	5.5	5.5	5.5
LiCl	15	14	14	13	11.5
$KOOCCH_3$	–	23.4	23.1	22.5	21.6
$CaCl_2$	40	33.5	33	32.5	32
$Ca(NO_3)_2$	61	56	–	50.5	–
NaCl	75.5	75.5	75.3	75.1	75
KCl	88	86	85.3	85	83.5
KH_2PO_4	95	95	–	95	–

replicates) placed on a layer of cotton wool moistened with deionized water. An embryo was considered as germinated when the radicle had elongated by 2–3 mm. Germination was scored daily for 7 d and the results presented are the means of the germination percentages obtained in 8 replicates ±SE as a function of time.

Quantification of temperature effects on sunflower embryo dormancy loss

Temperature effects on sunflower embryo dormancy status during storage were simulated using a simple population-based model. The three main steps required to develop the model involved: (i) establishing a thermal time equation for after-ripening, taking into account the natural variation within a seed population; (ii) introducing changes of germination speed and synchronicity induced by after-ripening (two possibilities, called A and B described below, were tested); and (iii) testing the efficiency of the model by comparing experimental data to simulated ones. Steps 1 and 2 can be achieved by mathematically testing various hypotheses which are fully described below.

The model was based on the assumptions that dormancy levels vary within a seed population or a seed lot (Batlla and Benech-Arnold, 2010), and that temperature effects on dormancy status can be quantified using thermal-time equations (Allen *et al.*, 2007; Chantre *et al.*, 2009; Batlla and Benech-Arnold, 2010). This implies that each embryo in a population requires a certain thermal-time for dormancy release. Consequently, if dormancy levels vary within a population, thermal-time requirements for dormancy loss should also vary within the population. Based on the above assumptions, the model was developed using a thermal-time equation which accounts for temperature effects on embryo dormancy status:

$$\theta_{AR}(g) = (T_{AR} - Tb_{AR}) \times t_{AR} \quad (1)$$

where θ_{AR} is after-ripening-thermal time in °Cd required for dormancy release for the fraction g of the population, T_{AR} is after-ripening temperature in °C, Tb_{AR} is the base temperature for after-ripening in °C (i.e. the temperature below which after-ripening does not occur), and t_{AR} is after-ripening time in d. To choose the best function to describe the distribution of θ_{AR} within a population, fits using four different distribution functions (normal, log-normal, Weibull, and exponential) were applied to experimentally obtained final germination percentages of embryos after-ripened at different temperatures for different time periods. The fits were compared using sum-of-squares when models had the same number of parameters or an extra-sum-of-squares F-test when models differed in the number of parameters (Motulsky and Ransnas, 1987; Motulsky and Christopoulos, 2004). During the fitting procedure the value of Tb_{AR} was included as a model variable (i.e. Tb_{AR} was allowed to vary when fitting each distribution equation).

If the distribution of θ_{AR} within a population is known, and how θ_{AR} accumulates in relation to temperature and time of after-ripening (equation 1), the fraction of embryos in which dormancy is alleviated at different temperatures and storage times can be predicted. However, in most species, seed dormancy loss is not only defined by changes in the fraction of the seed population capable of germinating at a certain temperature, but also by changes in germination speed and synchronicity (i.e. germination dynamics) (Gordon, 1973; Roberts and Smith, 1977; Favier, 1995). The most accepted definition of cardinal thermal-germination in the sub-optimal germination thermal-range (Garcia-Huidobro *et al.*, 1982; Covell *et al.*, 1986; Ellis *et al.*, 1986; Allen *et al.*, 2007) assumes that seeds in a population share a common germination base temperature (Tb_G) value, while thermal-time for seed germination (θ_G) is distributed within the seed population following a normal or log-normal distribution. According to this definition, changes in germination dynamics result from changes in: (A) the mean thermal-time required for seed germination θ_G (50) and its standard deviation σ_{θ_G}, and/or (B) the germination base temperature, Tb_G. Both possibilities (A and B) were tested and estimated for each cumulative-germination curve obtained for embryos after-ripened at the different temperatures for different time periods using the following equations:

$$\theta_G(g) = (T_G - Tb_G) \times t_g \quad (2)$$

where T_G is the germination temperature in °C and t_G the germination time in h,

$$G\% = G_{max} \times \Phi[(\theta_G(g) - \theta_G(50))/\sigma_{\theta_G}] \quad (3)$$

where $G\%$ is the percentage of embryo germination for a given θ_G, G_{max} is the maximum percentage of embryo to germinate, and Φ is the normal probability integral.

θ_G (50) and σ_{θ_G} were estimated for each cumulative-germination curve assuming a constant value for Tb_G during after-ripening. Conversely, Tb_G values were determined for each curve assuming constant values for $\theta_G(50)$ and σ_{θ_G}. G_{max} was limited to the maximum germination value observed in each cumulative-germination curve. The values for the parameters assumed constant in each case

were estimated from cumulative-germination curves of embryos considered fully non-dormant (12 weeks of after-ripening) at 5, 10, 15, and 20 °C. Germination rates (reciprocals of times estimated for each fraction) for sub-population 25th, 50th, and 75th were plotted against incubation temperature and data for each sub-population were fitted using a linear regression model. Tb_G was determined as the mean value of the three percentiles x-intercept. Linear regression equations were then recalculated for each subpopulation, but forced through Tb_G. $\theta_G(50)$ was estimated as the inverse slope of the regression equations for sub-population 50th. σ_{θ_G} was subsequently determined by adjusting a normal distribution function to the 25th, 50th, and 75th sub-populations θ_G values using GraphPad Prism 5 (GraphPad Software, San Diego, USA). The relative accuracy of both possibilities (changes in A or B, excluding simultaneous changes in both parameters) to simulate changes in germination dynamics (germination velocity and synchronicity) during sunflower seed dormancy loss was assessed using the Akaikes Information Criterion (AIC) (Burnham and Anderson, 1998; Motulsky and Christopoulos, 2004). Changes in germination dynamics were then introduced in the model by regressing changes in A or B to θ_{AR} accumulation during after-ripening.

Best values for model parameters (Tb_a and λ) and parameters associated with germination dynamics ($\theta_G(50)$, σ_{θ_G}, and Tb_G) were obtained by a non-linear least-squares curve-fitting method using an optimization program (Premium Solver Platform 7.0; Frontline Systems, Inc). This program optimizes parameters to maximize the fit of simulated values with experimentally recorded values. Optimization was performed by an iterative technique using a quasi-Newton optimization algorithm (Nocedal and Wright, 1999). The criterion used to obtain the best values for the parameters was minimum root mean square error (RMSE) between simulated and experimentally obtained data.

To evaluate model functioning, the fraction variance accounted for by the model was calculated as:

$$R^2 = 1 - \frac{\sum (y_{obs} - y_{sim})^2}{\sum (y_{obs} - \bar{y}_{sim})^2} \quad (4)$$

where y_{obs} is the observed value and y_{sim} is the simulated value. An R^2 value of 1 indicates a perfect fit of the model to the observed data.

Water sorption studies

Whole seeds were equilibrated at 5, 15, and 25 °C over saturated salt solutions giving RH values ranging from 1% to 95 % (Table 1). After equilibration, water contents, expressed on a dry weight (dw) basis were determined in excised embryonic axes and cotyledons by heating material at 105 °C for 2 d.

The following sorption model, adapted from the D'Arcy and Watt model (D'Arcy and Watt, 1970), was used to fit sorption data at 15 °C and to determine both seed tissue (axis and cotyledons) sorption characteristics, using non-linear least square regression as described in Dussert *et al.* (1999):

$$WC = K' + c(p/p_0) + \frac{kk'(p/p_0)}{1 - k(p/p_0)}$$

where WC is the tissue water content (expressed in g of absorbed water g^{-1} dry weight), p/p_0 is the relative vapour pressure (water activity), K', c, k, and k' are specific parameters. The first term describes sorption of strong binding sites, the second term relates to weak binding sites, and the third term describes sites where water condenses on molecules (multimolecular sorption). Non-linear regression was performed using the Statistica software (Statsoft, USA).

K' N/M; $cN/(Mp_0)$, and k' N/M were used for calculating the number of strong sorption sites, the number of weak sorption sites and the number of multimolecular sites, respectively, where N is the Avogadro number, M the gram molecular weight of water, and p_0 is 1.819 kPa at 16 °C.

Van't Hoff analyses (Atkins, 1982) were carried out to calculate the apparent sorption enthalpy ΔH_{sorp} at given MCs. Isochores interpolated from isotherms at 5, 15, and 25 °C were drawn in a range of MCs at 0.01 g H2O g–1 dw intervals. The slopes of regression lines between ln(RH/100) and 1/T were used to calculate ΔHsorp according to the equation:

$$\delta \mathrm{In}(\mathrm{RH}/100)/\delta(1/T) = \Delta H_{sorp}/R$$

where T is the temperature in Kelvin, R the ideal gas constant (8.3143 J K^{-1} mol^{-1}), and ΔH_{sorp} the apparent sorption enthalpy at a given MC.

Results

Effect of MC and temperature on embryo dormancy release

Table 2 shows the effects of relative humidity and temperature during after-ripening on the subsequent embryo germination, evaluated after 7 d at 10 °C. At harvest, sunflower embryos did not germinate at 10 °C, but they progressively became able to germinate fully at this temperature after 12 weeks of after-ripening at room temperature (data not shown, see Oracz *et al.*, 2007). Relative humidity and temperature of after-ripening strongly affected the kinetics of dormancy release. There was no constant and linear relationship between increasing RH, i.e. seed MC, increasing temperature, and alleviation of dormancy. At low RHs (until *c.* 33%) dormancy release was faster at 15 °C than at 30 °C. Conversely, at higher RHs (>75%), dormancy was alleviated faster at higher temperatures (25 °C and 30 °C). Figure 1 shows that the optimal MC for seed dormancy release, measured after 3 weeks of after-ripening at various RHs shown in Table 2, increases with temperature. When temperature increased by 5 °C, the

Table 2. Germination after 7 d at 10 °C of embryos placed at various relative humidities (RH) and temperatures for different durations of after-ripening

Exact RHs for each temperature are shown in Table 1.

Range of RH (%) (and saturated salt solution)	Duration of after-ripening (weeks)	Germination (%) after7 d at 10 °C of seeds after-ripened at			
		15 °C	20 °C	25 °C	30 °C
5.5	3	60±8.9	33±2.8	43±11.3	7±5.3
($ZnCl_2$)	4	50±2.8	48±0	18±2.8	20±5.5
23.4 to 21.6	3	96±0	90±2.8	80±0	68±4.0
($KOOHCH_3$)	4	98±2.6	98±1.8	72±11.3	62±8.5
	5	98±7.4	98±5.6	87±0	66±2.8
33.5 to 32	1	Nd	80±11.3	77±2.8	52±5.6
($CaCl_2$)	2	98±2.8	96±5.5	96±0	67±3.0
	3	98±2.8	98±2.8	94±4.2	48±3.0
	4	100±0	100±0	98±4.2	76±5.5
	5	100±0	100±0	100±0	58±8.5
75.5 to 75	1	Nd	24±6.6	34±15.0	35±16.9
(NaCl)	2	48±22.6	42±3.8	50±3.3	83±8.5
	3	50±6.3	63±11.3	86±9.0	89±11.3
	4	60±5.6	68±10.0	96±5.5	98±2.8
	5	44±0	70±8.5	94±5.0	96±0
86.0 to 83.5	1	14±8.5	22±8.5	20±10.1	42±3.0
(KCl)	2	31±5.6	47±3.0	54±2.8	78±8.9
	3	33±5.6	74±16.9	85±2.0	90±2.2

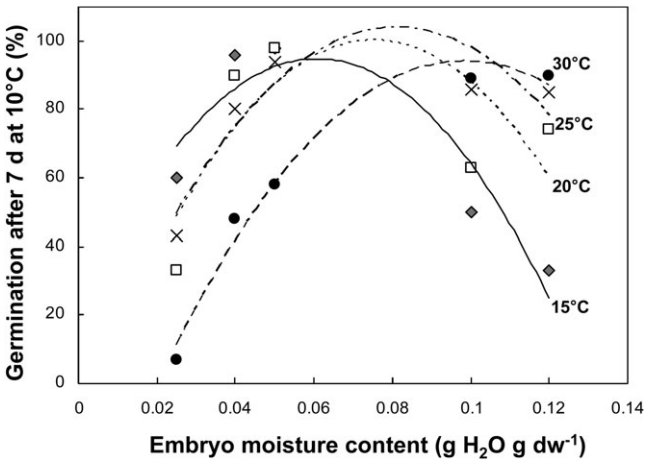

Fig. 1. Germination after 7 d at 10 °C of embryos previously stored for 3 weeks at 15 °C (black diamonds), 20 °C (crosses), 25 °C (white squares), and 30°C (black circles) at various relative humidities (see Table 2) which produced the indicated moisture contents.

optimal MC for dormancy alleviation increased by approximately 0.01 g H_2O g^{-1} dw.

Arrhenius plots express the relationship between MC and temperature of after-ripening on the subsequent embryo germination. The Arrhenius plots in Fig. 2 were constructed using data obtained after 3 weeks of after-ripening. When ln(germination) is plotted against reciprocal temperature $1/T$, a straight line is obtained at any MC with excellent fits

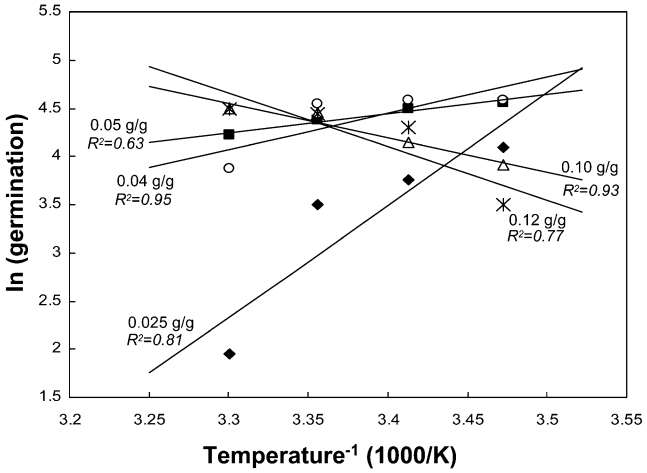

Fig. 2. Arrhenius plot of embryo dormancy release, where ln(germination), determined after 7 d at 10 °C, is plotted against the inverse after-ripening temperature [Temperature^{-1} (1000/K)]. Embryo moisture content during after-ripening and R^2 values of the linear regression lines are indicated within the graph. After-ripening lasted for 3 weeks.

as indicated by the correlation coefficients (Fig. 2). However, the relationship between germination and $1/T$ is negative at low MCs (0.025–0.05 g H_2O g^{-1} dw) and becomes positive when MC reaches 0.1 g H_2O g^{-1} dw. This indicates that the activation energy is negative below 0.1 g H_2O g^{-1} dw and becomes positive above this value. Similarly, the temperature coefficient Q_{10} between 15 °C and 30 °C ranged from 0.3 to 0.6 when seed MC was below 0.1 g H_2O g^{-1} dw, but from 1.5 to 1.9 when MC was higher than 0.1 g H_2O g^{-1} dw (data not shown).

Quantification of temperature effects on sunflower embryo dormancy release

A temperature-driven quantitative model was developed using cumulative-germination data for embryos equilibrated at *c.* 75% and 85% RH (i.e. embryo MCs were 0.1 and 0.12 g H_2O g^{-1} dw, respectively) because the fast rate of dormancy release observed for seeds equilibrated at *c.* 33% and at *c.* 22 % RH (i.e. when embryo MCs were 0.05 and 0.04 g H_2O g^{-1} dw, respectively) caused a lack of sufficient intermediate final percentage germination values for most of the tested storage temperatures (Table 2). For example, for embryos equilibrated at *c.* 33% RH, almost 80% germination was observed just after 1 week of storage at 20 °C, while after 3 weeks of storage germination values were ~90% for embryos equilibrated at 22% RH and stored at 15 °C and 20 °C. Germination data for seeds equilibrated at *c.* 75% and 85% RH were analysed together based on the fact that temporal changes in percentage germination for seeds stored at the different temperatures were statistically insignificant (*F*-test; $P > 0.05$) using a global fitting procedure (Motulsky and Christopoulos, 2004).

Our first objective was to find a good fit for the after-ripening of the population of dormant sunflower embryos.

From the fourth thermal after-ripening time (θ_{AR}) distributions tested (see Materials and methods), the Weibull distribution presented the lower sum-of-squares (data not shown). However, as the fit of the exponential distribution was not significantly different from the Weibull distribution (*F*-test (1,31); P=0.94), the exponential distribution was chosen because it is a simpler model. Therefore, it is possible to express the final germination percentage of embryos (i.e. G_{max}) for a certain quantity of accumulated θ_{AR} as follows:

$$G_{max} = (1-\exp(-\lambda \times \theta_{AR}(g))) \times 100 \quad (5)$$

where λ is the rate parameter (i.e. the germination percentage per unit of accumulated θ_{AR}).

Using equation 5, the optimum value for λ was determined to be 0.004643, and the optimum value for Tb_{AR} (equation 1) was 8.17 °C. This shows that after-ripening of dormant sunflower embryos is prevented at temperatures below *c*. 8 °C, at least within the range of MCs used to design the model. Replacing best-fit values in equations 5 and 1 leads to equations 6 and 7 that can be used to predict embryo dormancy alleviation as a function of accumulated thermal time:

$$G_{max} = (1-\exp(-0.004643 \times \theta_{AR}(g))) \times 100 \quad (6)$$

$$\theta_{AR}(g) = (T_{AR} - 8.17°C) \times t_{AR} \quad (7)$$

Equation 7 produced a good fit for the observed data (R^2=0.85: RMSE 9,6) and was used in Fig. 3, which clearly shows how the embryo fraction capable of germinating at 10 °C increases according to the accumulation of θ_{AR} units during storage.

Options A and B described in the Materials and methods were then assessed in order to integrate in the model changes in germination dynamics that occur during after-ripening. Changing germination parameters $\theta_G(50)$ and σ_{θ_G} (option A) during seed after-ripening accounted more accurately for changes in germination dynamics than changing the value of the germination base temperature, Tb_G (option B) (difference in AIC=3, IR=4.49; 4.5 times more likely to be correct). Therefore, a regression was calculated for values obtained for $\theta_G(50)$ and σ_{θ_G} using option A against θ_{AR} accumulation calculated using equation 7 (Fig. 4A, B). The changes in both parameters were adequately described by adjusting the following negative exponential equations:

$$\theta_G(50) = 961.8 \times \exp(-0.006038 \times \theta_{AR}) + 568.6 \quad (8)$$

$$\sigma_{\theta_G} = 171.1 \times \exp(-0.005236 \times \theta_{AR}) + 93.17 \quad (9)$$

Finally, the performance of the developed model was tested. Cumulative-germination data obtained experimentally for embryos that had been after-ripened at different temperatures for different time periods were compared with simulated values obtained using equations 6 to 9. As shown in Fig. 5A, a very good correlation was obtained between

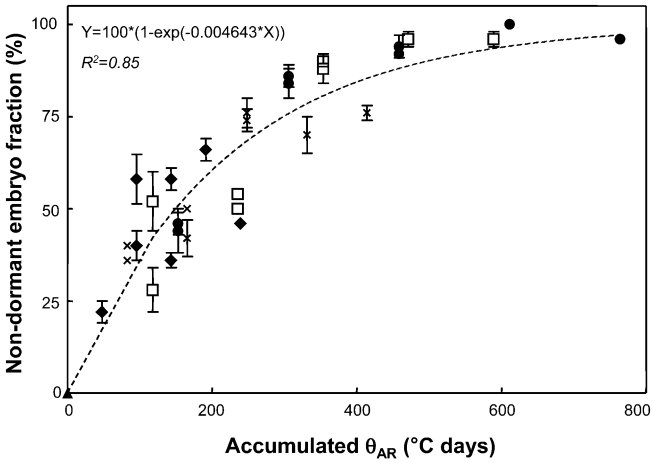

Fig. 3. Non-dormant embryo fraction (i.e. final germination percentage for embryos incubated at 10 °C) with MCs of 0.1 and 0.12 g H_2O g^{-1} dw stored at 15 °C (black diamonds), 20 °C (crosses), 25 °C (white squares), and 30 °C (black circles) for different time periods, and embryos of freshly harvested seeds (black triangle), plotted against after-ripening thermal-time (θ_{AR}) calculated with equation 7. The dashed line corresponds to simulation using equation 6 and 7. Vertical bars indicate standard error.

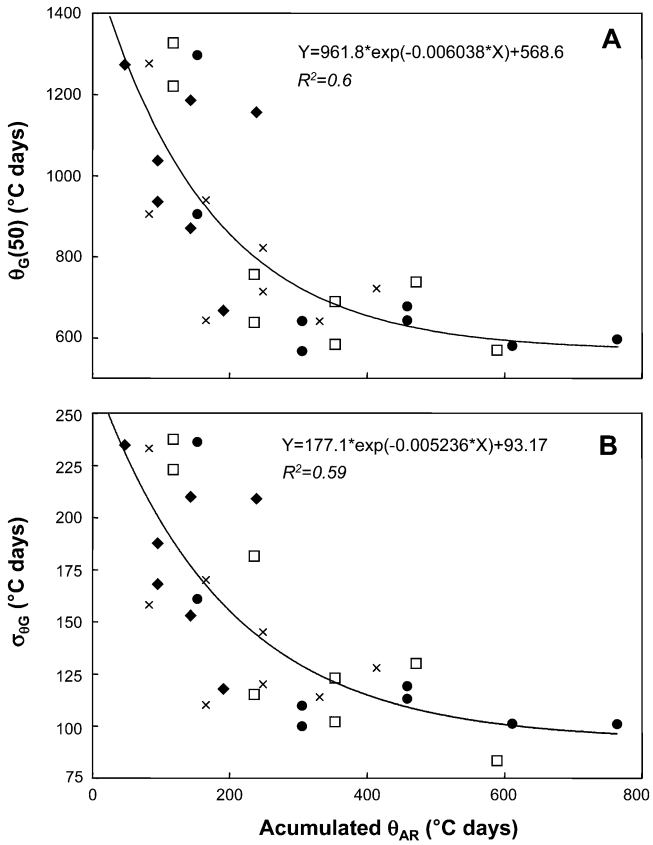

Fig. 4. (A) Estimated mean-thermal time of embryo germination [$\theta_G(50)$] and (B) standard deviations of thermal-time for embryo germination (σ_{θ_G}) with MCs of 0.1 and 0.12 g H_2O g^{-1} dw stored at 15 °C (black diamonds), 20 °C (crosses), 25 (white squares), and 30 °C (black circles) for different time periods, plotted against after-ripening thermal-time (θ_{AR}) calculated using equation 7. Solid lines correspond to fitted negative exponential equations.

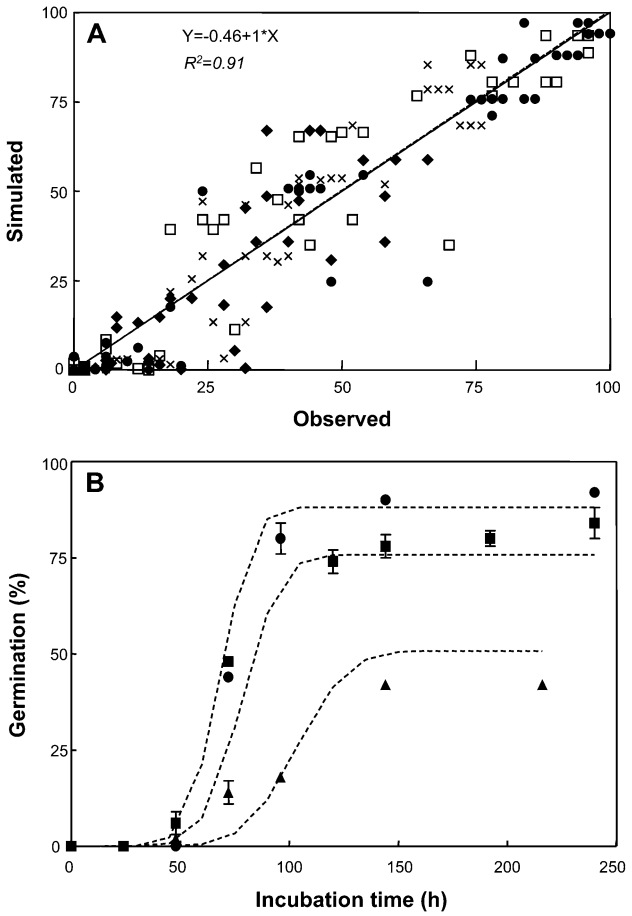

Fig. 5. (A) Relationship between observed germination percentages of embryos with MCs of 0.1 and 0.12 g H_2O g^{-1} dw stored at 15 °C (black diamonds), 20 °C (crosses), 25 °C (white squares), and 30 °C (black circles) for different time periods, and freshly harvested embryos (black triangles), and simulated germination percentages using equations 6 to 9. The solid line represents 1:1 relationship and the dashed line corresponds to the fitted linear equation. (B) Observed percentage germination kinetics for embryos with MCs of 0.12 g H_2O g^{-1} dw stored at 30 °C for 1 (triangle), 2 (square), and 3 (circle) weeks. Dashed lines correspond to simulated dynamics using equations 6 to 9. Vertical bars indicate standard error.

simulated and measured data (R^2=0.91), showing a slope of 1 and a root mean square error of 9.9. Figure 5B shows an example of how the model can simulate and predict the germination of embryos after-ripened for 1, 2, and 3 weeks at 30 °C, with a MC of 0.12 g H_2O g^{-1} dw.

Water sorption properties of dormant and non-dormant embryos

Water sorption isotherms were drawn using MCs of embryonic axes and cotyledons excised from dormant and non-dormant seeds equilibrated at various RHs (Table 1) at 5, 15, and 25 °C. Isotherms for 15 °C are shown as an example in Fig. 6. The relationship between RH and moisture content gave typical reverse sigmoid curves that can be divided into three regions, as indicated by the arrows within the plots: a first region below 10%, a second region ranging from *c*. 10–80%, and the last region above 80% RH (Fig. 6). The transition from regions 1 to 2 occurred at approximately 0.04 g H_2O g^{-1} dw in both the embryonic axis and the cotyledons and the transition from regions 2 to 3 was associated with *c*. 0.12 and 0.10 g H_2O g^{-1} dw in embryonic axes and in cotyledons, respectively (Fig. 6). At all RHs, the MCs of cotyledons were higher than those of embryonic axes (Fig. 6A, B). Isotherms show that non-dormant embryonic axes tended to bind more water than their dormant counterparts, particularly in the intermediate RH zone between 20% and 80% (Fig. 6A). By contrast, dormant cotyledons bound more water than the non-dormant ones (Fig. 6B).

Sorption data were used to investigate water properties in dormant and non-dormant tissues. Water sorption isotherms of dormant and non-dormant axes and cotyledons at 5, 15, and 25 °C were used to calculate the sorption enthalpy (ΔH_{sorp}) using van't Hoff plots (Fig. 7). These former were linear between 5 °C and 25 °C and their slopes, i.e. ΔH_{sorp}, decreased when MC increased (Fig. 7A). This is also shown in Fig. 7B and C, demonstrating that $-\Delta H_{sorp}$ increased dramatically when embryo MC decreased. The increase of $-\Delta H_{sorp}$ occurred at *c*. 0.08 g H_2O g^{-1} dw in dormant axes but only below 0.05 g H_2O g^{-1} dw in non-dormant ones (Fig. 7B, see arrows within the graph). This clearly shows that at any MC within the range typically used for sunflower seed storage, i.e. from 0.04 to 0.05 g H_2O g^{-1} dw, the values of $-\Delta H_{sorp}$ are much higher in dormant than in non-dormant axes (Fig. 7B). In dormant and non-dormant cotyledons $-\Delta H_{sorp}$ values increased when their MC was lower than *c*. 0.07 g H_2O g^{-1} dw (Fig. 7C). The maximum $-\Delta H_{sorp}$ values differed in dormant and non-dormant axes and reached *c*. 0.55 and 0.3 KJ mol^{-1} water, respectively (Fig. 7B). However, they were similar in dormant and non-dormant cotyledons and close to 0.25–0.3 KJ mol^{-1} water (Fig. 7C).

Sorption data obtained at 15 °C (Fig. 6) were fitted using a simplified D'Arcy and Watt model. The goodness of the fit was very satisfactory for both cotyledons and axes (Fig. 8). Using this model it was possible to estimate the parameters *K*', *c*, *k*, and k' and to calculate the number of sorption sites in each of the three binding regions (Table 3). Dormancy alleviation in the dry state mainly resulted in a dramatic increase in the number of weak sorption sites in embryonic axes which rose from *c*. 9×10^{20} g^{-1} dw to more than 17×10^{20} g^{-1} dw, when the number of multimolecular sorption sites decreased from 4.20 to 1.21×10^{20} g^{-1} dw (Table 3). In cotyledons seed after-ripening was associated with a decrease in strong and weak sorption sites and an increase in multimolecular sorption sites (Table 3).

Discussion

Sunflower seed dry after-ripening is associated with a widening of the thermal conditions allowing germination, as already shown by various authors (Corbineau *et al.*, 1990;

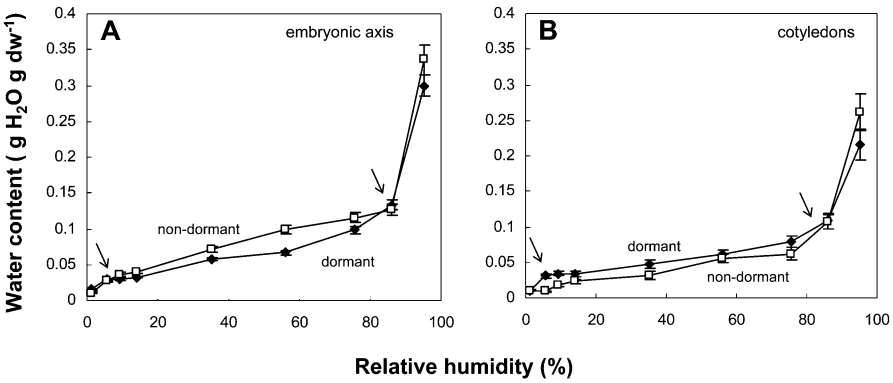

Fig. 6. Water sorption isotherms measured at 15 °C of axes (A) and cotyledons (B) excised from dormant and non-dormant embryos. Arrows within graphs indicate limits of regions of water binding (see text). Mean ±standard deviation of three measurements each of 15 organs.

Oracz *et al.*, 2007). After *c.* 2 months of dry storage, non-dormant naked seeds, i.e. embryos, became able to germinate fully at temperatures below 15 °C, which prevented their germination immediately after seed shedding. Our previous data indicated that sunflower dry after-ripening is associated with a marked increase in ROS content, and that this increase is prevented when seeds are stored in conditions that did not permit dormancy alleviation (Oracz *et al.*, 2007). The new set of data provided here demonstrates the close relationship between temperature and relative humidity during dry after-ripening and the rate of embryo dormancy alleviation. Within the ranges of MCs tested here (0.025–0.12 g H_2O g^{-1} dw), dormancy was progressively alleviated. However, at a given MC, the efficiency of dormancy removal depended on temperature. Our results are in agreement with previously published data showing that conversion to a non-dormant state occurs within the range of *c.* 0.05–0.2 g H_2O g^{-1} dw (Leopold *et al.*, 1988; Foley, 1994; Probert, 2000; Steadman *et al.*, 2003). In sunflower seeds, dormancy alleviation was not fully prevented at very low MCs, such as 0.025 g H_2O g^{-1} dw, at least when temperature ranged from 15–20 °C, but it was slow and incomplete (Table 2). Contrary to data reported for other species, there was no constant and linear relationship between temperature, relative humidity, and dormancy alleviation. It is shown that a complex relationship exists between these parameters in sunflower seeds, for example, the optimum embryo MC for dormancy release varies with temperature, and vice versa (Table 2; Fig. 1). The dependency of the rate of dry after-ripening on both temperature and seed MC is demonstrated by the Arrhenius plots (Fig. 2) and by calculation of Q_{10} values. Both approaches showed that a MC of 0.1 g H_2O g^{-1} dw is the critical value for the rate of dormancy alleviation and suggest that the reactions involved in dormancy alleviation may differ with seed MC. Below this value, the rate of dormancy alleviation decreases with increasing temperature suggesting a negative activation energy. Although negative activation energies are rather unusual, they have been associated with reactions involving unstable reactive chemical species, which tend to be degraded at high temperatures. For example, this is the case of the oxidation of nitric oxide by dioxygen (Olson *et al.*, 2002) and for the addition of hydroxyl radicals to aromatic molecules (Cheney, 1996). This is particularly interesting because our previous results demonstrated that dormancy alleviation at low MC, i.e. below 0.1 g H_2O g^{-1} dw, was associated with the production of ROS, most of which are very unstable molecules (Oracz *et al.*, 2007). Therefore, the present data set is in agreement with our biochemical results and confirms that the reactions involved in ROS generation at low MC are non-enzymatic. Auto-oxidation of lipids is favoured at very low MC and can, in turn, generate reactive free radicals (Labuza, 1980). Above 0.1 g H_2O g^{-1} dw, the rate of dormancy alleviation increased with temperature (Fig. 2), which is similar to the data already obtained for the seeds of other species (reviewed by Probert, 2000) and with the conceptual metabolic theory of ecology (Brown *et al*,. 2004). This quantitative theory emphasizes that the temperature dependence of biochemical processes governs survival and growth at all levels of organization, from individual to population. Therefore, we postulate that a mechanism involving active metabolism is involved in dormancy alleviation above 0.1 g H_2O g^{-1} dw. Due to its metabolic component, this mechanism is activated by temperature, which explains that the rate of after-ripening increases with temperature. We also propose that above this threshold MC, ROS, which are essential for sunflower seed dormancy release (Oracz *et al.*, 2007, 2009), will be produced by metabolic activities rather than auto-oxidative processes. Respiration, NADPH oxidases, peroxidases, and amine oxidases could all contribute to ROS production (Bailly *et al.*, 2008). Interestingly, Kibinza *et al.* (2006) showed that, in sunflower seeds, ATP levels changed when MCs reached 0.10 g H_2O g^{-1} dw, suggesting that metabolic activities occurred at this apparent low MC. ROS production during storage of dormant sunflower embryos at various MCs been previously reported (Oracz *et al.*, 2007) and associated with dormancy release. Although our approaches do not allow us to distinguish between non-enzymatic or enzymatic production of ROS, our data suggest that two different processes are involved in dormancy release and that they depend on embryo MC.

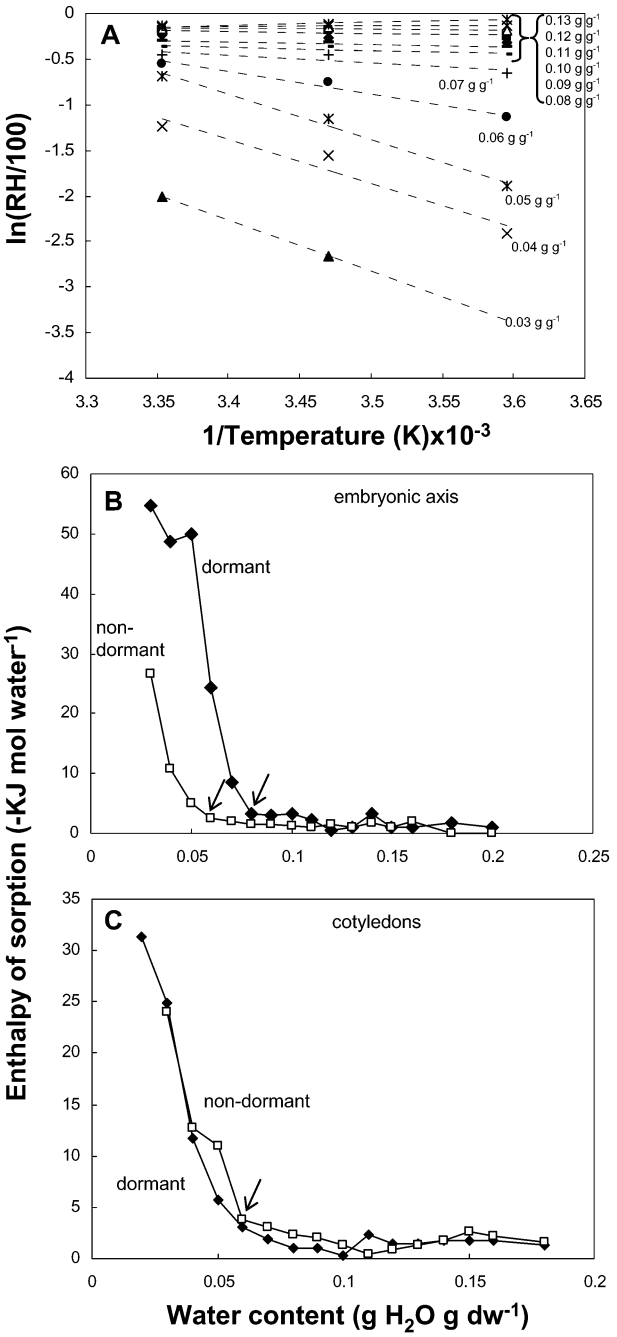

Fig. 7. (A) van't Hoff plots, obtained from water sorption isotherms, as shown in Fig. 7, of axes excised from dormant embryos. Axes MCs are indicated on the regression lines. (B, C) Relationship between water content of axes (B) and cotyledons (C) excised from dormant and non-embryos and the apparent water sorption enthalpy (ΔHsorp), calculated from the slopes of van't Hoff isochors similar to those given in (A). Arrows within (B) and (C) show the onset of the $-\Delta H$sorp increase.

In the present work a population-based threshold model and an optimization procedure were used to quantify the effect of after-ripening temperature on dormancy release for sunflower embryos stored at MCs above 0.1 g H_2O g^{-1} dw (i.e. the MC threshold value above which dormancy release could be explained by the effect of temperature on embryo metabolic activity). The model was not only capable of simulating changes in the fraction of embryos capable of germinating at 10 °C with acceptable accuracy (Fig. 3), but also to account for changes in germination dynamics (germination speed and synchronicity) during the dormancy loss process (Fig. 5). The model parameters obtained indicate that dormancy release for sunflower embryos with a MC above 0.1 g H_2O g^{-1} dw took place at temperatures above 8 °C (i.e. the threshold value for the accumulation of θ_{AR}, Tb_{AR} was 8.17 °C), and that the higher the after-ripening temperature above this value, the higher the dormancy loss rate. This value is relatively higher than those previously reported for the accumulation of θ_{AR} in other species: for example, 5.4 °C in *Lolium rigidum* (Steadman *et al.*, 2003) and 0 °C in *Bromus tectorum* (Bauer *et al.*, 1998). The effect of after-ripening temperature on dormancy loss was quantified using a thermal-time approach. Thermal-time equations have been successfully used to model temperature effects on dormancy loss in seeds of many species, for example, *Polygonum aviculare* (Batlla and Benech-Arnold, 2003, 2004, 2005), *Bromus tectorum* (Bauer *et al.*, 1998), *Elymus elymoides* (Meyer *et al.*, 2000), *Lolium rigidum* (Steadman *et al.*, 2003), *Lithospermum arvense* (Chantre *et al.*, 2009), and *Vitis* spp. (Wang *et al.*, 2009), showing the efficiency of this approach for predicting seed dormancy changes in response to temperature. The model was based on the assumption that θ_{AR} varies within the seed population, and in the present work this distribution was best accounted for by an exponential model, although a Weibull distribution gave similar results. This is shown in Fig. 3, in which a positive exponential equation gave a good description of how the fraction of the non-dormant embryo population increased as a consequence of the accumulation of θ_{AR} units. The exponential distribution of θ_{AR} within the embryo population implies that a relatively large fraction of embryos requires low θ_{AR} values for dormancy alleviation, while a relatively small fraction requires high θ_{AR} values for dormancy release. This type of response is consistent with previously reported dormancy loss kinetics, where a large fraction of the population rapidly becomes non-dormant, while a minor fraction requires extended time periods for dormancy release. For example, an exponential decrease of base water potential for seed germination during dormancy loss was reported by Batlla and Benech-Arnold (2004) for *P. aviculare* seeds and by Gianinetti and Cohn (2007) for red rice (*Oryza sativa*) seeds. However, a linear decrease in dormancy-related parameters has also been reported (Batlla and Benech-Arnold, 2003; Bauer *et al.*, 1998). A similar model based on the distribution of thermal-time required for dormancy release within a seed population was recently proposed by Wang *et al.* (2009) for moist stratification in grape seeds. However, stratification thermal time for dormancy release was assumed to be log-normally distributed within the seed population. Increases in germination speed and synchronicity observed during dormancy loss in sunflower seeds were introduced in the model by allowing $\theta_G(50)$ and σ_{θ_G} to vary, and fixing the value for Tb_G. Although changing $\theta_G(50)$ and σ_{θ_G} gave a better description

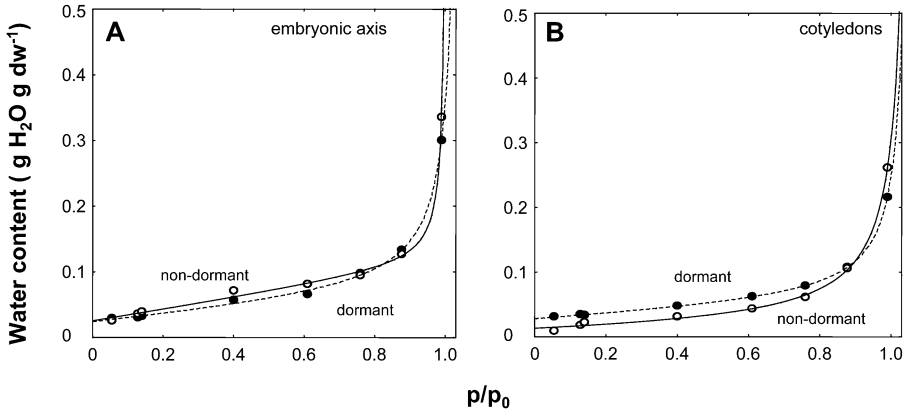

Fig. 8. Observed seed water contents (circles) at various relative vapour pressures (p/p_0) and fitted patterns (lines) of the simplified water sorption model of D'Arcy and Watt at 15 °C for axes (A) and cotyledons (B) excised from dormant and non-dormant embryos. Equations of the fitted curves are as follows: $y=(0.02418)+(0.049181)\times x+(0.957152)\times(0.012564)\times x/(1(0.957152)\times x)$ dormant axes; $y=(0.025397)+(0.094832)\times x+(0.994261)\times(0.003611)\times x/(1-(0.994261)\times x)$, non-dormant axes; $y=(0.028115)+(0.032127)\times x+(0.946626)\times(0.010466)\times x/(1-(0.946626)\times x)$, dormant cotyledons; $y=(0.013098)+(0.013446)\times x+(0.944572)\times(0.016282)\times x/(1-(0.944572)\times x)$, non-dormant cotyledons.

Table 3. Specific parameters (K', c, k, k') of the simplified water sorption model and number of sorption sites, calculated from these coefficients, in axes and cotyledons of dormant and non-dormant embryos

R^2 values indicated in the table refer to the equations shown Fig. 8.

	Dormant axes	Non-dormant axes	Dormant cotyledons	Non dormant cotyledons
K'	0.02418	0.02539	0.02811	0.01309
c	0.04918	0.09483	0.03212	0.01314
k	0.95715	0.99426	0.94662	0.94457
k'	0.01256	0.00361	0.01046	0.01628
R^2 fit	0.9986	0.9978	0.9999	0.9984
Strong sorption sites $\times 10^{20}$ g^{-1} dw	8.09	8.49	9.40	4.38
Weak sorption sites $\times 10^{20}$ g^{-1} dw	9.09	17.52	5.94	2.43
Multimolecular sorption sites $\times 10^{20}$ g^{-1} dw	4.20	1.21	3.50	5.44

of variations in germination dynamics than changing Tb_G, changes in the latter parameter during dormancy loss cannot be ruled out. Changes in $\theta_G(50)$ and σ_{θ_G} were described adjusting negative exponential equations, showing that, as in many other species, changes in the fraction of non-dormant seeds are accompanied by an increase in germination speed and synchronicity (Favier, 1995; Vleeshouwers, 1998; Wang *et al.*, 2009). To our knowledge this is the first attempt to quantify the effect of temperature on dormancy release in sunflower seeds. As pointed out previously, this model was produced considering the effects of temperature on the rate of dormancy release of embryos stored with 0.1 and 0.12 g H_2O g^{-1} dw. However, as shown by germination data (Table 2), embryo MC greatly interacts with storage temperature to affect the dormancy loss kinetics of stored seeds. This indicates that both factors, MC and temperature, should be taken into account to model the effect of storage temperature on sunflower dormancy loss for a broader set of storage conditions. Unfortunately, this was not possible in the present study because dormancy alleviation was too fast at low MC. This also suggests that attention should be paid to seed MC when developing models to predict the effect of after-ripening temperature on seed dormancy loss.

The sorption curves obtained with sunflower axes and cotyledons displayed a typical triphasic pattern as already observed for seeds of various species (Vertucci and Leopold, 1987) (Fig. 6). The shape of the isotherms and the RHs (and corresponding MCs) at which the transitions occurred from water-binding regions 1 to 2 and 2 to 3 are very similar to those found for other oilseeds such as peanut (Vertucci and Roos, 1990), *Arabidopsis* (Hay *et al.*, 2003) and tobacco (Manz *et al.*, 2005). In all cases embryonic axes bind significantly more water than cotyledons because they contain fewer lipids. With regard to dormancy, the isotherms showed that dry after-ripening (at 20 °C and 70% RH for 12 weeks) is associated with changes in water status within the seed tissues, especially in embryonic axes which bind more water in the intermediate zone (20–80% RH) of the isotherms when they are non-dormant (Fig. 6). Such changes have already been observed in seeds but only became apparent when comparing primed and unprimed seeds (Sun *et al.*, 1997; Nagajaran *et al.*, 2005) rather than dormant and non-dormant seeds. By contrast, in tobacco,

the moisture sorption isotherms of freshly harvested seeds and after-ripened seeds did not differ (Manz *et al.*, 2005). These results are confirmed when calculating adsorption enthalpies at specific MCs according to van't Hoff analyses of isotherms (Fig. 7). Values of ΔH_{sorp} were roughly similar to those reported for other orthodox seeds (Vertucci and Leopold, 1987; Leopold *et al.*, 1988; Foley, 1994) and, as shown by Vertucci and Leopold (1987), ΔH_{sorp} values were more negative for axes than cotyledons. Changes in ΔH_{sorp} values with MC were similar in dormant and non-dormant cotyledons but the moisture content at which $-\Delta H$sorp abruptly increased was higher in dormant axes than in non-dormant axes (Fig. 7B). The higher values of ΔHsorp and the highest affinity of water binding at intermediate MCs (0.05–0.075 g H_2O g^{-1} dw) for dormant axes reveal that after-ripening drastically affects water sorption properties in axes, but not in cotyledons. In addition, the modified d'Arcy and Watt equation showed that the affinity of weak binding sites (c) was the major factor to be affected by dry after-ripening in embryonic axes (Table 3). Consequently, the number of weak sorption sites was much higher in non-dormant than in dormant axes (Table 3). The shift towards more and weaker bound water in tissues of embryonic axes seems to be associated with dormancy alleviation. It is important to note that the changes in water properties are tissue specific and concern only the growing part of the seed, i.e. the embryonic axis. As pointed out previously, dormancy alleviation is associated with increased ROS accumulation and oxidation of proteins and lipids (Oracz *et al.*, 2007) and that these oxidative processes may be associated with the observed changes in water status during after-ripening. It has been shown in other systems, for example, wheat gluten, that protein oxidation resulted in increased water sorption (Cherian and Chinachoti, 1997). Moreover, sorption isotherms of aged sunflower seeds, which contain high concentrations of ROS and oxidized compounds (Bailly *et al.*, 1996), show that aged sunflower seeds tend to bind more water than non-aged seeds (data not shown). Proteins are probably one of the major sites of water sorption in sunflower seeds because they are present at high concentrations (i.e. around 25% of seed dry weight), whereas lipids, the major storage compounds of sunflower seeds, are hydrophobic and exclude water. Protein oxidation results in the formation of disulphide bonds that can, in turn, induce conformational changes in proteins (Buchanan and Balmer, 2005; Colville and Kranner, 2010) and subsequently increase interactions with water (Cherian and Chinachoti, 1997). The consequences of increased water sorption in non-dormant embryonic axes need to be understood with respect to molecular mobility. Sorption enthalpy has been related to molecular mobility and structural stability in amorphous solids such as glasses (Zhang and Zografi, 2000; Ballesteros and Walters, 2007). Under our experimental conditions (maximum temperature, 30 °C; maximum MC, 0.12 g H_2O g^{-1} dw), sunflower seeds displayed a cytoplasmic glassy state (Lehner *et al.*, 2006). The ability of non-dormant axes to bind more water will result in loosening of molecular connections within the glassy matrix because water is a plasticizer of glasses (Walters, 1998). Glasses restrain molecular mobility, thus decreasing the speed of chemical reactions and protecting cellular structures from deleterious changes (Burke, 1986; Walters, 1998). In amorphous solids, a high relative ΔH_{sorp} value reflects higher viscosity and restricted molecular mobility. Changes in this value during dry after-ripening as well as changes in the c value in the D'Arcy and Watt equation therefore suggest that dormancy release is associated with lower viscosity and higher molecular mobility. Moreover, because sunflower seed tissues contain many hydrophobic oil bodies, the MC of the non-lipid fraction most likely reached higher values than those determined experimentally (Kibinza *et al.*, 2006). Together, these results suggest that metabolic reactions may progressively become possible during after-ripening, as a consequence of altered water-binding properties. This could explain why gene expression has been observed during after-ripening in *Nicotiana tabacum* (Leubner-Metzger, 2005), *Nicotiana plumbaginifolia* (Bove *et al.*, 2005), *Arabidopsis* (Cadman *et al.*, 2006), barley (Leymarie *et al.*, 2007), and sunflower (El-Maarouf-Bouteau *et al.*, 2007). However, there is still some debate about the occurrence of active transcription in the dry state under conditions where water is apparently not available for biochemical reactions. Leubner-Metzger (2005) proposed that hydrated pockets within cells or tissues of the seeds would allow transcription. We propose that non-enzymatic oxidation (Oracz *et al.*, 2007) could lead to a progressive decrease in water binding and an increase in cellular mobility thus allowing active transcription.

In conclusion, it has been demonstrated that the complex relationship between temperature and MC governs the nature of the mechanisms involved in sunflower embryo dormancy release during dry storage. The temperature dependency of after-ripening has been modelled for the first time for this species and we wish to draw attention to the MC dependency of the temperature-dependent after-ripening process and its implications for the development of predictive dormancy models. Our data highlight the central role of water organization and binding properties, especially for desiccated tissues such as orthodox seeds, and provide new insights into the underlying mechanisms of anhydrobiosis.

Acknowledgements

The authors wish to thank Dr Ilse Kranner (Seed Conservation Department, Royal Botanic Gardens, Kew, UK) for her critical review of this work and for her useful comments.

References

Allen PS, Benech-Arnold RL, Batlla D, Bradford KJ. 2007. Modeling of seed dormancy. In: Bradford K, Nonogaki H, eds. *Seed development, dormancy and germination*, Vol. 27. Oxford: Blackwell Publishing, 72–112.

Atkins PW. 1982. *Physical chemistry*. San Francisco: WH Freeman and Company.

Bailly C, Benamar A, Corbineau F, Côme D. 1996. Changes in superoxide dismutase, catalase and glutathione reductase activities as related to seed deterioration during accelerated aging of sunflower seeds. *Physiologia Plantarum* **97,** 104–110.

Bailly C, El-Maarouf-Bouteau H, Corbineau F. 2008. From intracellular signaling networks to cell death: the dual role of reactive oxygen species in seed physiology. *Comptes Rendus Biologies* **331,** 806–814.

Bair NB, Meyer SE, Allen PS. 2006. A hydrothermal after-ripening time model for seed dormancy loss in *Bromus tectorum* L. *Seed Science Research* **16,** 17–28.

Ballesteros D, Walters C. 2007. Water properties in fern spores: sorption characteristics relating to water affinity, glassy states, and storage stability. *Journal of Experimental Botany* **58,** 1185–1196.

Batlla D, Benech-Arnold RL. 2003. A quantitative analysis of dormancy loss dynamics in *Polygonum aviculare* L. seeds. Development of a thermal time model based on changes in seed population thermal parameters. *Seed Science Research* **13,** 55–68.

Batlla D, Benech-Arnold RL. 2004. Seed dormancy loss assessed by changes in *Polygonum aviculare* L. population hydrotime parameters. Development of a predictive model. *Seed Science Research* **14,** 277–286.

Batlla D, Benech-Arnold RL. 2005. Changes in the light sensitivity of buried *Polygonum aviculare* seeds in relation to cold-induced dormancy loss: development of a predictive model. *New Phytologist* **165,** 445–452.

Batlla D, Benech-Arnold RL. 2006. The role of fluctuations in soil water content on the regulation of dormancy changes in buried seeds of *Polygonum aviculare* L. *Seed Science Research* **16,** 47–59.

Batlla D, Benech-Arnold RL. 2007. Predicting changes in dormancy level in weed seed soil banks: implications for weed management. *Crop Protection* **26,** 189–197.

Batlla D, Benech-Arnold RL. 2010. Predicting changes in dormancy level in natural seed soil banks. *Plant Molecular Biology* **73,** 3–13.

Bauer MC, Meyer SE, Allen PS. 1998. A simulation model to predict seed dormancy loss in the field for *Bromus tectorum* L. *Journal of Experimental Botany* **49,** 1235–1244.

Bove J, Lucas P, Godin B, Oge L, Jullien M, Grappin P. 2005. Gene expression analysis by cDNA-AFLP highlights a set of new signaling networks and translational control during seed dormancy breaking in *Nicotiana plumbaginifolia*. *Plant Molecular Biology* **57,** 593–612.

Brown JH, Gillooly JF, Allen AP, Savage VM, West GB. 2004. Toward a metabolic theory of ecology. *Ecology* **85,** 1771–1789.

Buchanan BB, Balmer Y. 2005. Redox regulation: a broadening horizon. *Annual Review of Plant Biology* **56,** 187–220.

Buitink J, Hoekstra FA, Leprince O. 2004. Biochemistry and biophysics of tolerance systems. In: Black M, Pritchard HW, eds. *Desiccation and survival in plants: drying without dying*. Wallingford: CAB International, 293–318.

Burke MJ. 1986. The glassy state and survival of anhydrous biological systems. In: Leopold AC, ed. *Membranes, metabolism and dry organisms*. Ithaca, New York: Cornell University Press, 358–363.

Burnham KP, Anderson DR. 1998. *Model selection and inference: a practical information-theoretic approach*. New York: Springer-Verlag.

Cadman CSC, Toorop PE, Hilhorst HWM, Finch-Savage WE. 2006. Gene expression profiles of Arabidopsis Cvi seeds during dormancy cycling indicate a common underlying dormancy control mechanism. *The Plant Journal* **46,** 805–822.

Chantre G, Batlla D, Sabbatini M, Orioli G. 2009. Germination parameterization and development of an after-ripening thermal-time model for primary dormancy release of *Lithospermum arvense* seeds. *Annals of Botany* **103,** 1291–1301.

Christensen M, Meyer SE, Allen PS. 1996. A hydrothermal time model of seed after-ripening in *Bromus tectorum* L. *Seed Science Research* **6,** 147–153.

Cheney BV. 1996. AM1 calculations on reactive oxygen species. Part 1. Analysis of hydroxyl radical reactions. *Journal of Molecular Structure (Theochem)* **364,** 219–237.

Cherian G, Chinachoti P. 1997. Action of oxidants on water sorption, ^{2}H nuclear magnetic resonance mobility, and glass transition behavior of gluten. *Cereal Chemistry* **74,** 312–317.

Colville L, Kranner I. 2010. Desiccation tolerant plants as model systems to study redox regulation of protein thiols. *Plant Growth Regulation* DOI: 10.1007/s10725-010-9482-9.

Corbineau F, Bagniol S, Côme D. 1990. Sunflower (*Helianthus annuus* L.) seed dormancy and its regulation by ethylene. *Israel Journal of Botany* **39,** 313–325.

Covell S, Ellis RH, Roberts EH, Summerfield RJ. 1986. The influence of temperature on seed germination rate in grain legumes. 1. A comparison of chickpea, lentil, soybean and cowpea at constant temperatures. *Journal of Experimental Botany* **37,** 705–715.

D'Arcy RL, Watt IC. 1970. Analysis of sorption isotherms of non-homogeneous sorbents. *Transactions of the Faraday Society* **66,** 1236–1245.

Dussert S, Chabrillange N, Engelmann F, Hamon S. 1999. Quantitative estimation of seed desiccation sensitivity using a quantal response model: application to nine species of the genus *Coffea* L. *Seed Science Research* **9,** 135–144.

El-Maarouf-Bouteau H, Job C, Job D, Corbineau F, Bailly C. 2007. ROS signaling in seed dormancy alleviation. *Plant Signaling and Behaviour* **2,** 362–364.

Ellis RH, Covell S, Roberts EH, Summerfield RJ. 1986. The influence of temperature on seed germination rate in grain legumes. 2. Intraspecific variation in chickpea (*Cicer arietinum* L.) at constant temperatures. *Journal of Experimental Botany* **37,** 1503–1515.

Favier JF. 1995. A model for germination rate during dormancy loss in *Hordeum vulgare*. *Annals of Botany* **76,** 631–638.

Finch-Savage WE, Leubner-Metzger G. 2006. Seed dormancy and the control of germination. *New Phytologist* **171,** 501–523.

Finkelstein R, Reeves W, Ariizumi T, Steber C. 2008. Molecular aspects of seed dormancy. *Annual Review of Plant Biology* **59,** 387–415.

Foley ME. 1994. Temperature and water status of seeds affect afterripening in wild oat (*Avena fatua*). *Weed Science* **42,** 200–204.

Garcia-Huidobro J, Monteith JL, Squire GR. 1982. Time, temperature and germination of pearl millet (*Pennisetum typhoides* S & H). I. Constant temperature. *Journal of Experimental Botany* **33,** 288–296.

Gianinetti A, Cohn MA. 2007. Seed dormancy in red rice. XII. Population-based analysis of afterripening with a hydrotime model. *Seed Science Research* **17,** 253–271.

Gillooly JF, Brown JH, West GB, Savage VM, Charnov EL. 2001. Effects of size and temperature on metabolic rate. *Science* **293,** 2248–2251.

Gordon AG. 1973. The rate of germination. In: Heydecker W, ed. *Seed ecology*. London: Butterworths, 391–410.

Hay FR, Mead A, Manger K, Wilson FJ. 2003. One-step analysis of seed storage data and the longevity of *Arabidopsis thaliana* seeds. *Journal of Experimental Botany* **54,** 993–1011.

Kebreab E, Murdoch A. 1999. A quantitative model for loss of primary dormancy and induction of secondary dormancy in imbibed seeds of *Orobanche* spp. *Journal of Experimental Botany* **50,** 211–219.

Kibinza S, Vinel D, Côme D, Bailly C, Corbineau F. 2006. Sunflower seed deterioration as related to moisture content during ageing, energy metabolism and active oxygen species scavenging. *Physiologia Plantarum* **128,** 496–506.

Labuza TP. 1980. The effect of water activity on reaction kinetics of food deterioration. *Food Technology* **34,** 36–41.

Lehner A, Corbineau F, Bailly C. 2006. Changes in lipid status and glass properties in cotyledons of developing sunflower seeds. *Plant and Cell Physiology* **47,** 818–828.

Leopold AC, Glenister R, Cohn MA. 1988. Relationship between water content and afterripening in red rice. *Physiologia Plantarum* **74,** 659–662.

Leubner-Metzger G. 2005. β-1,3-Glucanase gene expression in low hydrated seeds as a mechanism for dormancy release during tobacco after-ripening. *The Plant Journal* **41,** 133–145.

Leymarie J, Bruneaux E, Gibot-Leclerc S, Corbineau F. 2007. Identification of transcripts potentially involved in barley seed germination and dormancy using cDNA-AFLP. *Journal of Experimental Botany* **58,** 425–437.

Manz B, Müller K, Kucera B, Volke B, Leubner-Metzger G. 2005. Water uptake and distribution in germinating tobacco seeds investigated *in vivo* by nuclear magnetic resonance imaging. *Plant Physiology* **138,** 1538–1551.

Meyer SE, Debaene-Gill SB, Allen PS. 2000. Using hydrothermal time concepts to model seed germination response to temperature, dormancy loss, and priming effects in *Elymus elymoides*. *Seed Science Research* **10,** 213–223.

Motulsky HJ, Christopoulos A. 2004. *Fitting models to biological data using linear and nonlinear regression. A practical guide to curve fitting*. New York: Oxford University Press.

Motulsky HJ, Ransnas LA. 1987. Fitting curves to data using nonlinear regression: a practical and nonmathematical review. *FASEB Journal* **1,** 365–374.

Nagajaran S, Pandita VK, Joshi DK, Sinha JP, Modi BS. 2005. Characterization of water status in primed seeds of tomato (*Lycopersicon esculentum* Mill.) by sorption properties and NMR relaxation times. *Seed Science Research* **15,** 99–111.

Nocedal J, Wright SJ. 1999. *Numerical optimization*. New York: Springer-Verlag.

Olson LP, Kuwata KT, Bartberger MD, Houk KN. 2002. Conformation-dependent state selectivity in O–O cleavage of ONOONO: an 'inorganic cope rearrangement' helps explain the observed negative activation energy in the oxidation of nitric oxide by dioxygen. *Journal of the American Chemical Society* **124,** 9469–9475.

Oracz K, El-Maarouf-Bouteau H, Farrant J, Cooper K, Belgazhi M, Job C, Job D, Corbineau F, Bailly C. 2007. ROS production and protein oxidation as a novel mechanism of seed dormancy alleviation. *The Plant Journal* **50,** 452–465.

Oracz K, El-Maarouf-Bouteau H, Kranner I, Bogatek R, Corbineau F, Bailly C. 2009. The mechanisms involved in seed dormancy alleviation by hydrogen cyanide unravel the role of reactive oxygen species as key factors of cellular signalling during germination. *Plant Physiology* **150,** 494–505.

Pritchard HW, Tompsett PB, Manger KR. 1996. Development of a thermal time model for the quantification of dormancy loss in *Aesculus hippocastanum* seeds. *Seed Science Research* **6,** 127–135.

Probert RJ. 2000. The role of temperature in the regulation of seed dormancy and germination. In: Fenner M, ed. *Seeds. The ecology of regeneration in plant communities*. Oxon: CABI Publishing, 261–292.

Roberts EH, Smith RD. 1977. Dormancy and the pentose phosphate pathway. In: Khan AA, ed. *The physiology and biochemistry of seed dormancy and germination*. Amsterdam: Elsevier/North-Holland Biomedical Press, 385–411.

Steadman KJ. 2004. Dormancy release during hydrated storage in *Lolium rigidum* seeds is dependent on temperature, light quality, and hydration status. *Journal of Experimental Botany* **55,** 929–937.

Steadman KJ, Crawford AD, Gallagher RS. 2003. Dormancy release in *Lolium rigidum* seeds is a function of thermal after-ripening time and seed water content. *Functional Plant Biology* **30,** 345–352.

Sun WQ. 2004. Methods for the study of water relations under desiccation stress. In: Black M, Pritchard HW, eds. *Desiccation and survival in plants: drying without dying*. Wallingford: CAB International, 47–91.

Sun WQ, Yoh DCY, Ong CM. 1997. Correlation of modified water sorption properties with the decline of storage stability of osmotically-primed seeds of *Vigna radiata* (L.) Wilczek. *Seed Science Research* **7,** 391–397.

Vertucci CW, Farrant JM. 1995. Acquisition and loss of desiccation tolerance. In: Kigel J, Galili G, eds. *Seed development and germination*. New York: Marcel Dekker, 237–271.

Vertucci CW, Leopold AC. 1987. Water binding in legume seeds. *Plant Physiology* **85,** 224–231.

Vertucci CW, Roos EE. 1990. Theoretical basis of protocols for seed storage. *Plant Physiology* **94,** 1019–1023.

Vertucci CW, Roos EE. 1993. Theoretical basis of protocols for seed storage. II. The influence of temperature on optimal moisture levels. *Seed Science Research* **3,** 201–213.

Vleeshouwers LM. 1998. The effect of seed dormancy on percentage and rate of germination in *Polygonum persicaria*, and its

relevance for crop–weed interaction. *Annals of Applied Biology* **132,** 289–299.

Walters C. 1998. Understanding the mechanisms and kinetics of seed aging. *Seed Science Research* **8,** 223–244.

Wang WQ, Song SQ, Li SH, Gan YY, Wu JH, Cheng HY. 2009. Quantitative description of the effect of stratification on dormancy release of grape seeds in response to various temperatures and water contents. *Journal of Experimental Botany* **12,** 397–406.

Zhang J, Zografi G. 2000. The relationship between 'BET'- and 'Free Volume'-derived parameters for water vapor absorption into amorphous solids. *Journal of Pharmaceutical Sciences* **89,** 1063–1072.